Cell Transplantation
2019, Vol. 28(4) 400–412

DOI: 10.1177/0963689718823705
journals.sagepub.com/home/cll
SAGE

The Effect of iPS-Derived Neural Progenitors Seeded on Laminin-Coated pHEMA-MOETACl Hydrogel with Dual Porosity in a Rat Model of Chronic Spinal Cord Injury

Jiri Ruzicka[1], Nataliya Romanyuk[1], Klara Jirakova[1], Ales Hejcl[1], Olga Janouskova[2], Lucia Urdzikova Machova[1], Marcel Bochin[1,3], Martin Pradny[2], Lydia Vargova[1,3], and Pavla Jendelova[1,3]

Abstract

Spinal cord injury (SCI), is a devastating condition leading to the loss of locomotor and sensory function below the injured segment. Despite some progress in acute SCI treatment using stem cells and biomaterials, chronic SCI remains to be addressed. We have assessed the use of laminin-coated hydrogel with dual porosity, seeded with induced pluripotent stem cell-derived neural progenitors (iPSC-NPs), in a rat model of chronic SCI. iPSC-NPs cultured for 3 weeks in hydrogel in vitro were positive for nestin, glial fibrillary acidic protein (GFAP) and microtubule-associated protein 2 (MAP2). These cell-polymer constructs were implanted into a balloon compression lesion, 5 weeks after lesion induction. Animals were behaviorally tested, and spinal cord tissue was immunohistochemically analyzed 28 weeks after SCI. The implanted iPSC-NPs survived in the scaffold for the entire experimental period. Host axons, astrocytes and blood vessels grew into the implant and an increased sprouting of host TH^+ fibers was observed in the lesion vicinity. The implantation of iPSC-NP-LHM cell-polymer construct into the chronic SCI led to the integration of material into the injured spinal cord, reduced cavitation and supported the iPSC-NPs survival, but did not result in a statistically significant improvement of locomotor recovery.

Keywords

Chronic spinal cord injury, human induced pluripotent stem cells, neural progenitors, HEMA hydrogel, laminin, surface charge

Introduction

Spinal cord injury (SCI) is a complex event and involves primary and secondary injury mechanisms that are spatially and temporally specific. Primary injury refers to the destructive nature of the initial impact and the subsequent shearing, penetrating, and compressive forces that injure the fragile neural tissue. A cascade of processes, such as edema, lipid peroxidation, inflammation and excitotoxicity, cause oligodendroglial death and the demyelination of the surviving axons[1]. Distal axons subsequently degenerate, with corollary proximal axons unable to grow through the glial scar, due to inhibitory myelin fragments within the lesion site[2,3].

All of these pathologic processes potentiate gliosis, pseudocyst formation and vascular changes that remodel the spinal tissue in the chronic phase of injury, creating an inhibitory environment in the lesion[1]. This phase of SCI presents a major challenge to physicians and scientists and attracts the greatest research interest, as most patients remain in this phase for the rest of their lives. Despite several successful

[1] Department of Tissue Culture and Stem Cells, Institute of Experimental Medicine, CAS, Prague, Czech Republic
[2] Department of Polymer Networks and Gels, Institute of Macromolecular Chemistry, CAS, Prague, Czech Republic
[3] Department of Neurosciences, 2nd Faculty of Medicine, Charles University, Prague, Czech Republic

Submitted: May 24, 2018. Revised: December 7, 2018. Accepted: December 17, 2018.

Corresponding Author:
Jiri Ruzicka, Institute of Experimental Medicine, CAS, Videnska 1083, 14200, Prague, Czech Republic.
Email: jiri.ruzicka@iem.cas.cz

approaches in animal models toward functional recovery in SCI in the acute and subacute phases[4–8], effective strategies for the chronic phase of SCI have not yet been established. Therefore, the treatment of chronic SCI will likely require a multifactorial approach. This can include not only the replacement of the lost population of cells, but also artificial scaffolds to bridge the lesion cavity.

Stem and progenitor cells are particularly useful tools for regenerative medicine, since they have the ability to modify the lesion environment. Generally, they increase the levels of neurotrophic factors important for neuroprotection and neuroregeneration. As a result, axonal elongation and collateral sprouting, remyelination, synapse formation and reduced retrograde axonal degeneration can be observed[9]. Cell transplantation has been shown to be one of the most promising strategies to promote functional recovery in acute and subacute SCI[10–12]. Recently discovered induced pluripotent stem cells (iPSCs) have emerged as a promising new source of pluripotent stem cells for the treatment of different diseases. In 2006, Takahashi and Yamanaka[13] reported that fully differentiated cells could be simply and completely dedifferentiated into a pluripotent state by four defined factors (Oct4, c-Myc, Klf4 and Sox2) – iPSCs. This approach has since undergone many modifications including differentiation into neural derivatives. Human neural stem cells derived from iPSCs have already shown their strong potential in the experimental treatment of SCI[14–17]. Grafted cells survived and differentiated into a neural phenotype. Furthermore, their transplantation enhanced axonal sparing/regrowth and angiogenesis, and reduced astrogliosis. In our latest study, we compared human bone marrow mesenchymal stem cells (MSCs) and two types of neural progenitors (NPs), including cells from a human conditional fetal spinal line (SPC-01, c-mycERTAM technology), and human iPSC-derived neural progenitors (iPSC-NPs), in the treatment of rat balloon-induced spinal cord compression lesion. The use of iPSC-NPs to treat an acute SCI positively affected the majority of studied factors involved in spinal cord regeneration, such as glial scar formation, axonal sprouting, tissue sparing and cytokine levels. This cumulative effect resulted in an improved performance in advanced locomotor tests (flat beam test and rotarod), requiring better movement coordination.

Recently, we described the synthesis of the macroporous hydrogel containing two types of pores[18]. The preparation of dual-porosity gels based on poly(2-hydroxyethyl methacrylate), (pHEMA) is a simple method, which offers tailoring gel samples to various required shapes. Large pores of the order of tens of micrometers were generated by adding a solid porogen (fractionated particles of sodium chloride) to the polymerization mixture, which was subsequently washed out of the gel. Small pores of the order of micrometers were formed by the mechanism of reaction induced phase separation, caused by the addition of a diluent (1-dodecanol; DD) which is a precipitant for pHEMA. We found in vitro that double porous hydrogel is more suitable for cell proliferation, when compared with gels with one type of pore. Larger pores are suitable for cell adhesion and expansion, while smaller pores enable the diffusion of nutrients and cannot be occupied by the cells. The aim of this study was to test modified pHEMA hydrogel by a positive charged co-monomer (2-(methacryloyloxy) ethyl trimethylammonium chloride; MOETACl), with two types of pores coated with laminin, as a bridging material and/or as a stem cell carrier for the treatment of a chronic model of spinal cord lesion. For stem cells, iPSC-NPs were chosen due to their positive effect in the treatment of acute SCI[19,20]. An effective influence of MOETACl on cell proliferation was previously described[21].

In this study, we have evaluated the effect of laminin-coated pHEMA-MOETACl (LHM) hydrogel seeded with iPSC-NPs in chronic rat SCI. As a model of SCI, a balloon-induced spinal cord compression lesion was chosen. We studied the effect of this cell-polymer construct on behavioral recovery, the integration of the graft into the damaged spinal cord, and the fate of the implanted stem cells and their influence on endogenous tissue elements.

Materials and Methods

Materials

LHM hydrogel preparation. HEMA was purchased from Wichterle and Vacik Ltd. (Prague, Czech Republic), 1,2-ethylene dimethacrylate (EDMA), 1-dodecanol (DD), 2,2′-azobis (2-methylpropionitrile; AIBN) were purchased from Sigma-Aldrich and used without purification. Sodium chloride particles of the mesh 30–50 μm were obtained by sieving, using precise Retsch test sieves of the corresponding mesh sizes. MOETACl was prepared by the procedure described earlier[22].

Hydrogel was prepared by the procedure described earlier[18] using the mixture of HEMA (1 g), DD (1.5 g), EDMA (0.0275 g), AIBN (0.01 g), NaCl (7 g) and MOETACl (0.03 g). The mixture, with sodium chloride particles (7 g) was polymerized in a stainless steel mold at 70°C for 8 hours. After polymerization, the solvent, sol fraction, and salt template particles now embedded in polymerized gel, were washed out with ethanol (5×24 h), and the gels were then washed with distilled water (10×24 h). Prepared hydrogels were coated overnight with poly-L-ornithine 0.01% (Sigma-Aldrich, St. Louis, MO, USA), diluted 1:6 in distilled (DI) water for the cell culture media (Thermo Fischer Scientific, Waltham, MA, USA) at 37°C. The gels were then washed in DI water and coated with laminin, diluted in Dulbecco's modified Eagle medium (DMEM; Thermo Fischer Scientific) at a final concentration of 10 μg/ml for 2 h at 37°C.

Diffusion Parameters of the LHM Hydrogel

The extracellular space (ECS) diffusion parameters: volume fraction α (α=ECS/total tissue volume), tortuosity λ (λ^2=D/ADC, where D is the free diffusion coefficient and ADC is the apparent diffusion coefficient in the brain tissue) and non-

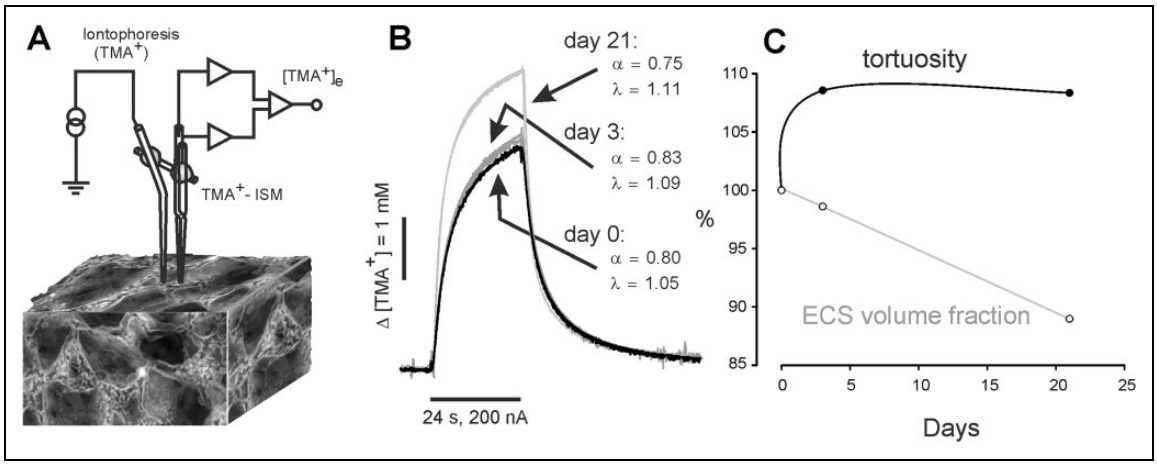

Fig. 1. Experimental set-up and representative TMA^+ diffusion curves in native gel, and 3 (3-d) and 21 days (3-w) after cell seeding. To stabilize the inter-tip distance of the electrode array, an iontophoretic micropipette and TMA^+-selective microelectrode (ISM) were glued together with dental cement (A). Note the increased curve amplitude reflecting the reduction of the ECS volume fraction α in 3-w hydrogel, already populated with cells (B). Development of the changes in the ECS volume fraction α and tortuosity λ, calculated as a percentage of their values in the native hydrogel, which were set to 100% (C). Note that an increase in tortuosity, indicating the production of diffusion barriers created, for example by cell processes, was already observed in 3-d hydrogel, while a significant decrease in the ECS volume fraction was present only in 3-w gel, after a robust stem cell proliferation.
ECS: extracellular space; ISM: ion-selective microelectrode; TMA: tetramethylammonium.

specific uptake k′ were investigated in the native hydrogel, and after stem cell seeding, using the real-time iontophoretic method [23]. Briefly, an extracellular marker such as the tetramethylammonium ion (TMA^+, MW=74.1 Da), was administered into the hydrogel by an iontophoretic pulse, and time-dependent changes in its local concentration were measured with a double-barreled TMA^+ ion-selective microelectrode (TMA^+ ISM). TMA^+ ISMs were prepared as described previously[24]. The tip of the ion-sensitive barrel was filled with a liquid ion exchanger for K^+ (Corning 477317 or IE 190 from World Precision Instruments, Sarasota, FL, USA), that is highly sensitive to TMA^+ ions; the rest of the barrel was backfilled with 150 mM TMA^+ chloride. The reference barrel contained 150 mM NaCl (Fig. 1A). The electrodes were calibrated using the fixed-interference method before each experiment, in a series of solutions of 150 mM NaCl+3 mM KCl, with the addition of the increasing concentrations of TMA chloride.

For a stabile array, spacing around 100 μm, the TMA^+ ISM was glued together with an ionophoretic micropipette in a parallel position by dental cement (Fig. 1A). Typical iontophoresis parameters were 20 nA bias current (continuously applied to maintain a constant transport number) and a +180 nA current step, with a 24 sec duration to generate the diffusion curve. The electrode array was first calibrated in 0.5% agar (Sigma-Aldrich), dissolved in a solution of 150 mM NaCl, 3 mM KCl and 1 mM TMACl, by which definition $\alpha=1$, $\lambda=1$ and $k`=0$ (free diffusion values). The diffusion curves obtained in agar were analyzed to yield the electrode transport number (n) and the free TMA^+ diffusion coefficient (D) by a curve fitting according to a modified diffusion equation, using the VOLTORO program (C. Nicholson, unpublished data). Measurements were then repeated at intervals 300–3100 μm deep inside the hydrogel. Knowing n and D, the parameters α and λ were calculated from the diffusion curves recorded in the hydrogel, using a nonlinear curve-fitting simplex algorithm[25]. In each experiment, x–y diffusion curves were obtained in various depths of one insertion track (n insertion per gel=5 ± 2) and the data were pooled (n tracks per insertion=6 ± 2); x–y tracks were performed in each hydrogel sample (n gels per experiment= $N^{0d}=5$, $N^{3d}=3$, $N^{21d}=4$). Typical diffusion curves obtained during the experiment are depicted in Fig. 1B)

Human iPSC-NPs and Seeding on Gels

The human iPSC line was derived from female human fetal lung fibroblasts (IMR90; ATCC, Manassas, VA, USA), transduced according to Yu et al., 2007[26], with a lentivirus-mediated combination of OCT4, SOX2, NANOG and LIN28 human cDNA (all prepared at I-Stem, Strasbourg, France). Clone selection, validation of the iPSC line and derivation of NPs are described in detail in Polentes et al[27]. Briefly, early NPs were produced in a low-attachment culture in the presence of Noggin (500 ng/ml) (R&D Systems, Minneapolis, MN, USA), the transforming growth factor-β pathway inhibitor SB 431542 (10 nM; Sigma-Aldrich), fibroblast growth factor 2 (FGF2) (10 μg/ml) and brain-derived neurotrophic factor (BDNF) (20 μg/ml; both from Pepro Tech, London, UK). Human iPSC-NPs were routinely cultured in tissue culture flasks coated with poly-L-ornithine (0.002% in distilled water) and laminin (10 μg/ml in DMEM: F12), both from Sigma. Growth media comprising DMEM: F12 and Neurobasal medium (1:1), B27 supplement (1:50), N2 supplement (1:100; GIBCO, Life Technologies, Eugene, OR, USA),

primocin (100 μg/ml; InvivoGen, San Diego, CA, USA), FGF (10 ng/ml), EGF (10 ng/ml) and BDNF (20 ng/ml; PeproTech, London, UK) was changed three times per week. iPSC-NPs were characterized by qPCR and FACS in previously published studies[19,27]. The cells expressed a low level of pluripotent markers (oct3/4, nanog, SSEA4, TRA1-60) and were positive for neural markers (SSEA1, CD133, CD24, CD29, CD56, and NF70). The cells were harvested and 3×10^5 of cells were seeded on gel samples approximately $3\times3\times3$ mm and incubated 3 weeks before implantation. The medium was changed three times per week.

Immunocytochemistry

After a 3-week incubation period, gels were fixed in 4% paraformaldehyde in phosphate-buffered saline (PBS) for 15 min. Prior to immunostaining, the fixed gels were washed three times in PBS. Gels were treated for 2 h at room temperature (RT) with normal goat serum (dilution 1:10; Sigma-Aldrich) and Triton X-100 (0.1%; Sigma-Aldrich) in 0.1 M PBS (45 min, RT) to block non-specific staining.

To identify iPSC-NPs and their differentiation, antibodies against nestin (mouse monoclonal IgG1, 1:100, Merk-Millipore, Billerica, MA, USA); neurofilament 160 kDa (NF-160, mouse monoclonal IgG1, 1:200, Sigma-Aldrich); glial fibrillary acidic protein (GFAP; mouse monoclonal IgG1 conjugated with Cy3, 1:800, Sigma-Aldrich); F-actin (Alexa-Fluor 568 phalloidin; fluorescently labeled toxin of *Amanita phalloides* with high-affinity and selective binding to a wide range of plant and animal F-actin, 1:400, Molecular Probes, Eugene, Oregon, USA), oligodendrocyte (rabbit polyclonal to OLIG2, 1:250, Sigma-Aldrich) and microtubule-associated protein 2 (MAP2; mouse monoclonal IgG1, 1:1000, Merk-Millipore).

To visualize primary antibody reactivity, appropriate secondary antibodies were used: goat anti-mouse IgG (H+L) Alexa-Fluor 594 (1:400; Life Technologies) and goat anti-rabbit IgG (H+L) Alexa-Fluor 594 (1:400; Life Technologies).

Each secondary antibody was diluted in 0.1 M PBS with normal goat serum (10%) and Triton X-100 (0.1%) for 2.5 h at 4°C, in dark. Additional nucleic acid staining was performed with 4′,6-diamidino-2-phenylindole (DAPI, 1:1000, Life Technologies). After immunostaining, gels were subsequently saturated with 10%, 20% and 30% solution of sucrose (aq) and cut in frozen mode (local temperature at −24°C) using sliding microtome to slides 60 μm thick. All the slides were washed with 0.1 M PBS and mounted using Aqua-Poly/Mount (Polysciences Inc., Warrington, PA, USA). Confocal images were taken with a Zeiss LSM 5 duo confocal microscope (Carl Zeiss AG, Oberkochen, Germany)

Animals

A total of 30, 10-week old male Wistar rats (300 g ± 10 g), have been used in our study. The animals were housed in pairs in internally ventilated cages (IVCs; Tecniplast, London, UK) in environmentally controlled rooms (22–24°C). At 5 weeks after SCI, hydrogel (n=10), iPSC-NP seeded hydrogel (n=11) or saline (n= 9) were implanted into the developed cavity. All animals underwent a series of behavioral tests prior to, and post transplantation. They were studied for 28 weeks after SCI. After the end of the study, the animals were used for the histology and immunohistochemistry analysis in order to detect the structural changes after SCI and the fate of the implanted cell-polymer construct.

SCI

According to the protocol from previous publications, a balloon compression model of SCI was performed. All surgical procedures were performed under sterile conditions. Anesthetic (3.5 vol. %, Forane, 300 ml/min) and analgesic (intramuscular injection, Rimadyl 50 μl) conditions were applied prior to surgery. The balloon of surgical 2-French Fogarthy catheter was inflated (15 μl) for 5 minutes to induce the SCI (level Th 8–9)[7,28]. To prevent post-surgical infection, an intramuscular injection of gentamicin (Lek Pharmaceutical, 5 mg/kg) was given daily for 10 days after SCI. Manual urinary bladder expression was performed twice a day to prevent urine retention. Prior to magnetic resonance imaging (MRI), the animals with SCI were randomly divided into three groups (controls, gel only, gel seeded with iPSC-NPs). At 5 weeks after SCI, the cavity in the injured spinal cord was localized by MRI scan, glial scar was resected and the cavity was filled with either gel or gel with iPSC-NP cells. The control group with SCI did not undergo any additional surgery. The MRI images were taken in order to guide hydrogel implantation, as after laminectomy the balloon-induced compression lesion is not discernible on the surface. The time point of 5 weeks was chosen according to our previous study, Hejcl et al.[29], where we showed that the cavities are formed 5 weeks after lesion induction. These cavities are visible on MRI scans as white hyperintense spots (Fig. 2A). Using MRI, the injured spinal cords with implanted with LHM hydrogel (with or without iPSC-NPs) were imaged in week 28 after SCI (before the end of the study). During the first 2 months, daily immunosuppression (cyclosporine A; 10 mg/kg) was given to all the animal groups, eliminating the effect of immunosuppression on SCI. Due to the cumulative effect, the immunosuppression was injected every second day after 2 months, and the dose was reduced to half every second month until the end of the study.

Tissue Processing

To analyze the effect of implanted cell-polymer construct on host spinal cord tissue, the animals were sacrificed 5 months after SCI. The rats were transcardially perfused with 4% paraformaldehyde in PBS. The spinal cords were removed and a 2 cm long segment with the lesion epicenter was post-fixed overnight, and then used for the histological and

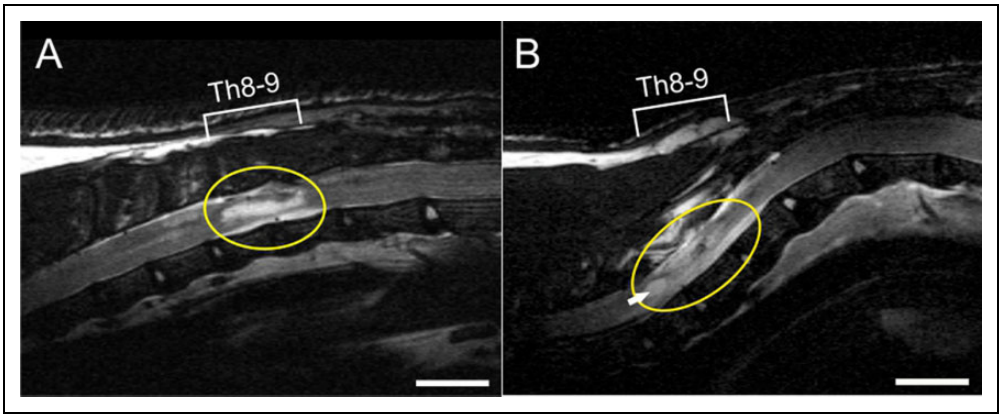

Fig. 2. (A) MRI scan of spinal cord lesion 5 weeks after SCI in rat (before hydrogel implantation). Lesion cavity is indicated by hyper-intensive signal (circle). The insertion of LHM hydrogel (with or without cells) was performed according to individual MRI scans. (B) LHM hydrogel seeded with cells (circle) adhered well to the host tissue; only a small cavity is visible at the rostral part of the implant (arrow). MRI scan was taken 28 weeks after SCI. Scale bar is 500 μm.
LHM: laminin-coated pHEMA-MOETACl; MRI: magnetic resonance imaging; SCI: spinal cord injury.

immunohistochemical analysis. In order to monitor the incorporation of the hydrogel, and the location, survival and differentiation of the implanted NPs, serial longitudinal sections (14 μm) of the spinal cord were prepared (Leica CM1850 cryostat, Leica Mikrosysteme GmbH, Vienna, Austria).

In order to identify the implanted human cells in the rat spinal cord, antibodies against human nuclei (HuNu, Merk-Millipore) or mitochondria (MTC02, Abcam, Cambridge, UK) were used. To identify the differentiation pattern of iPSC-NPs 28 weeks after implantation, antibodies against MAP2 (Abcam), cholinacetyltransferase (ChAT; ab68779 Abcam), Islet2, NKx6,1 (both DSHB, Iowa City, IA, USA), Calbindin, DOPA (both Abcam), and tyrosine hydroxylase (TH; Sigma-Aldrich) were used.

The infiltration of specific tissue elements into the cell-polymer construct was detected by antibodies against axons (NF200, Sigma-Aldrich), blood vessels (RECA, Abcam) and astrocytes (GFAP, Sigma-Aldrich).

To evaluate the density and distribution of TH-positive fibers in spinal cord tissue, histological samples stained for TH and DAPI were scanned by Zeiss Axio Scan.Z1. For image analysis and fiber counting, ZEN 2.3 lite software was used. To count the number of TH-positive fibers, the lesion area on the spinal cord pictures taken by the scanner was painted by the lines perpendicular to the rostral caudal axis at 1 mm distance from each other. TH-positive fibers which crossed the lines were marked and calculated by the software. Data were exported to Excel and statistical analysis was performed.

The reactivity of primary antibodies was visualized by secondary antibodies against goat anti-mouse IgG conjugated with Alexa-Fluor 488, or goat anti-rabbit IgG conjugated with Alexa-Fluor 594 (Molecular Probes). The immunohistochemical and histological analyzes were performed using a ZEISS AXIO Observer D1 microscope (Carl Zeiss) and Wizzard (Carl Zeiss) or ImageJ (NIH, Bethesda, MA, USA) software. To interpret the data set into graphical format, Excel 2010 (Microsoft, USA) and Corel DRAWx5 (Corel Corporation, Ontario, Canada) were used.

Behavioral Assessment

Basso, Beattie, and Bresnahan Test. Basic over-ground locomotion was assessed using Basso, Beattie, and Bresnahan (BBB) open field test[30]. Two independent examiners were scoring (0–21) the locomotor ability of injured rats in a circular arena for 5 minutes every third week for 28 weeks after SCI, starting 1 week before implantation.

Plantar Test. The plantar test was performed using hot plate apparatus (Ugo Basile, Comercio, Italy). A radiant thermal stimulus was applied to the surface of the hindlimb paw. The latency of the paw withdrawal was measured five times for each session, once per 3 weeks up until the end of the study. Hyperalgesia was defined as a significant decrease in latency of withdrawal.

Data Processing. The data from the behavioral study were processed using Excel (Microsoft) and Sigmastat 3.1 (Sistat Software Inc., San Jose, CA, USA) software. All the numbers are presented solely in the graphs and connected by trend curves.

Results

In Vitro Diffusion Parameters of iPSC-NP-Seeded LHM Hydrogel

We have shown in our previous studies that changes in the extracellular space (ECS) diffusion parameters reflect structural rebuilding and alterations in tissue morphology fairly accurately[25]. To assess how stem cell seeding affects the diffusion properties of the hydrogel, and thus its

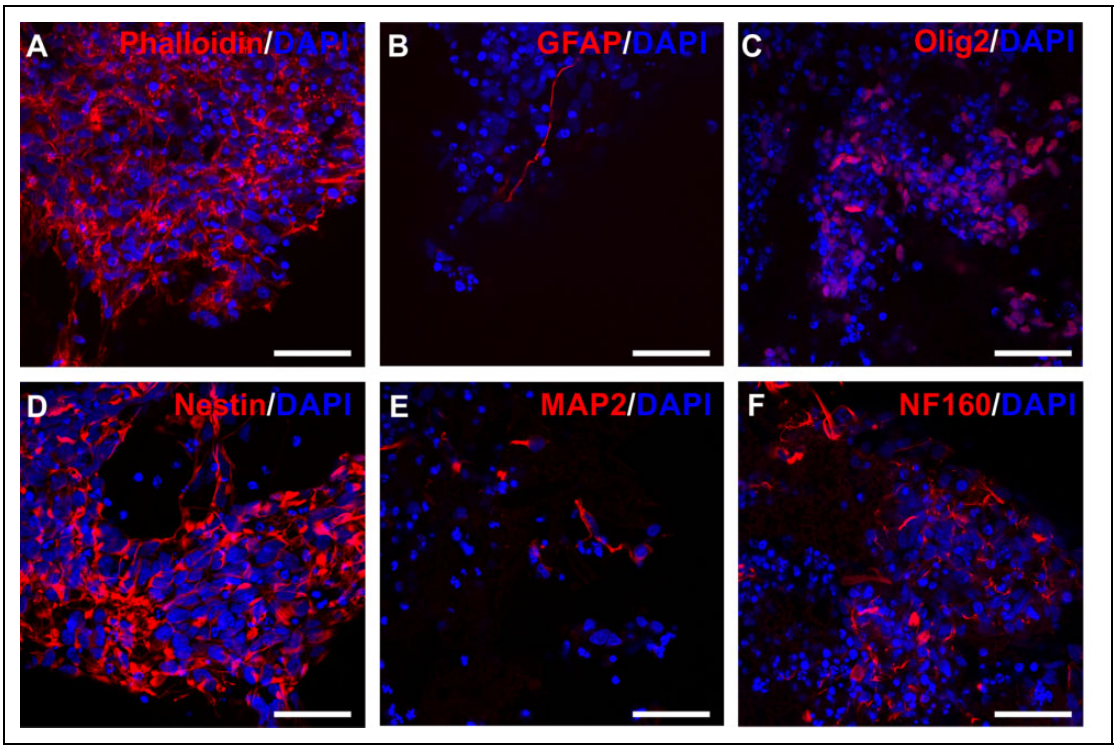

Fig. 3. Immunocytochemistry of iPSC-NPs in gel samples. IPSC-NPs were cultivated for 3 weeks in gels and stained for various markers. Phalloidin (A), GFAP (B), olig2 (C), nestin (D), MAP2 (E), NF160 (F) (red). Nuclei were stained with DAPI (blue). Scale bar is 50 μm. DAPI: 4', 6-2, dihydrochloride; GFAP: glial fibrillary acidic protein; iPSC-NP: induced pluripotent stem cell-derived neural progenitor; MAP2: microtubule-associated protein 2.

permeability for axonal ingrowth and movement of the nutrition and trophic factors, we measured the ECS diffusion parameters volume fraction α tortuosity λ in the hydrogel prior to, and 3 days and 3 weeks after stem cell seeding and cell growth (3-d and 3-w, respectively). Due to the dual porosity of the gel, diffusion parameters between different electrode tracks varied a lot, especially in the native gel and early after cell seeding. Three weeks after cell seeding, the gel was already populated with proliferating cells and the diffusion parameters were far more consistent. Diffusion parameters in the LHM hydrogel without cells were $\alpha=0.84\pm0.03$ and $\lambda=1.02\pm0.02$ ($n=24$, $N=5$, where n=number of tracks, N=number of hydrogel samples) and resemble the diffusion parameters in the medium with free diffusion, where by definition both α and λ equals 1. Proliferation of the cells in the 3-d gel did not lead to a significant change in α, but was accompanied by an increase in λ ($\alpha=0.83\pm0.03$ and $\lambda=1.11\pm0.01$, $n=31$, $N=3$). A significant decrease in α and stable λ was found in 3-w gels ($\alpha=0.75\pm0.02$ and $\lambda=1.11\pm0.01$, $n=44$, $N=4$; Fig. 1C).

The in Vitro Effect of LHM Hydrogel on iPSC-NP Survival and Differentiation

The cells were analyzed after 3 weeks of culturing in gels for various markers to show the cell density in gel, and the differentiation state in the phase of implantation into animals. Staining for actin, and neuroectodermal stem cell marker nestin showed cells with morphology of viable NPs. The cells grew in large clusters and spread deeply in the structure of the gel, and were not only on the surface. The cells did not show many signs of differentiation to astrocytes at this stage, as there was little GFAP positivity. More cells were positive for neural progenitor marker olig2, which is involved in oligodendrocyte and motor neuron differentiation. Staining against NF160 and MAP2 supports differentiation directed into neuronal lineage (Fig. 3).

Cavitation and Hydrogel Incorporation

In the control animals with SCI receiving saline only, the center of the lesion was atrophic with astrocytic scarring (Fig. 4A, detail A1). Residual axons were present in the remaining tissue (Fig. 4B). Both seeded or unseeded gel implants adhered well to the endogenous tissue, however they were surrounded with glial scar regardless of iPSC-NPs presence (Fig. 5E, F). An MRI scan 28 weeks after SCI, confirmed the incorporation of the implant into the host tissue. Only a small cavity was present on the rostral side of the gel (Fig. 2B). No ingrowth of axons or astrocytes into the gel implant was detected in the unseeded gels (Fig. 5A, E), however blood vessels infiltrated even the gels without cells (Fig. 5C, detail C1).

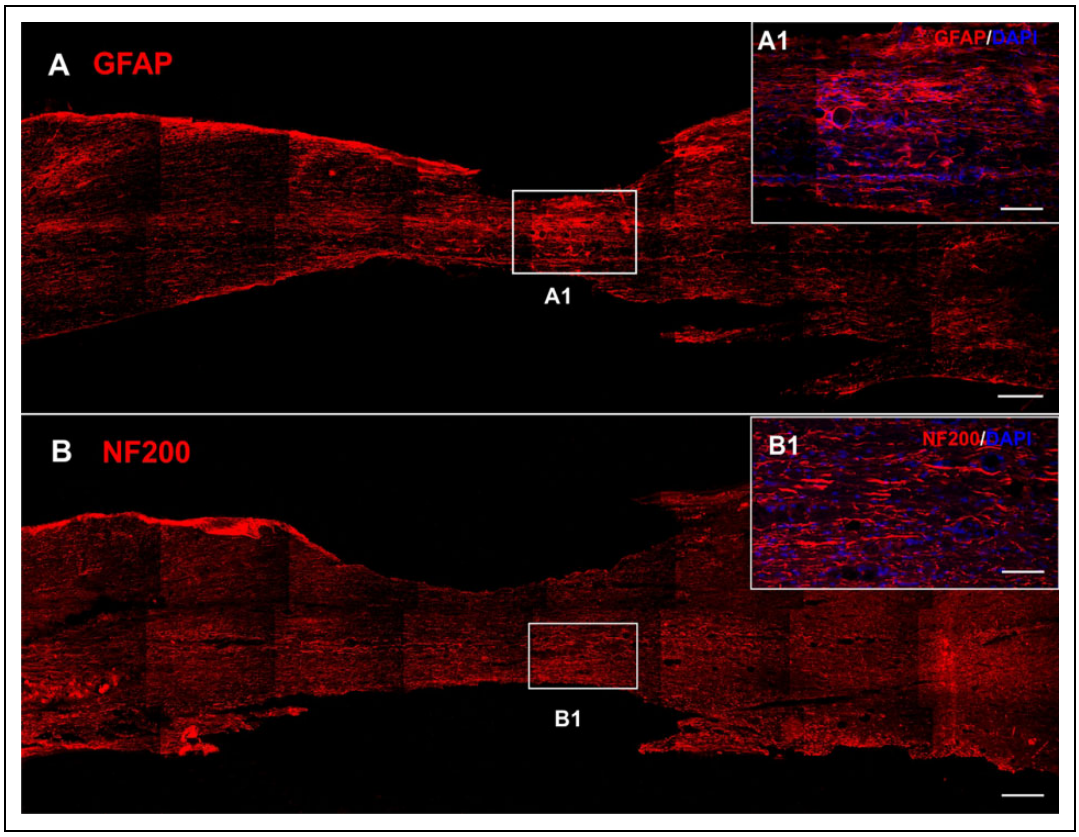

Fig. 4. Immunohistochemistry showing the chronic lesion injected with saline 28 weeks after SCI. Tissue in the lesion center was atrophic with glial scar (GFAP, red, A, detail A1). Axons were present in the remaining tissue (NF200, red B, detail B1). Nuclei were stained with DAPI (blue). Scale bars are 500 μm (A, B), 20 μm (A1, B1).
DAPI: 4′,6-diamidino-2-phenylindole; GFAP: glial fibrillary acidic protein; SCI: spinal cord injury.

Cell-polymer constructs were infiltrated with endogenous axons (Fig. 5B, detail B1, 2) and blood vessels (Fig. 5D, detail D1, 2). GFAP-positive astrocytes were found in the close vicinity of the cell-polymer construct, as well as the surrounding hydrogel edges as part of the glial scar (Fig. 5F, detail F1, 2).

Stem Cell Fate After Implantation

Implanted iPSC-NPs survived within the hydrogel implant, as well as in the spinal tissue throughout the whole study. IPSC-NPs were found in the LHM scaffold 28 weeks after implantation, however, the environment of the hydrogel did not support further growth, differentiation and maturation. Cells which migrated outside the hydrogel, and were in contact with the host tissue mostly showed neuronal morphology, and were positive for NF200 and MAP2 (Fig. 6). However, we did not observe any further advanced maturation or differentiation, since none of the cells were positive for mature motor neuron markers, such as ChAT, Islet2, NKx6.1 or calbindin.

The Effect of the Implant on TH^+ Neurons

The implanted cell-polymer construct significantly affected not only the infiltration of endogenous tissue elements in the bridged cavity, but also increased the sprouting of TH^+ axons in the injured region, as well as in the surrounding host tissue (Fig. 7). The implanted LHM hydrogel facilitated axonal sprouting when compared with the saline-treated animals. This effect was more enhanced when iPSC-NPs were present in the LHM material (Fig. 7A, B, E).

Behavioral Analysis

At 5 weeks after lesion induction, prior to hydrogel implantation, the animal scores varied between 6 and 13. Due to the high variability of the lesion at the time of LHM implantation, we did not see any significant improvement in functional outcome (Fig. 8A) in any of the treated animal groups. However, 75% of the animals with implanted cell-polymer construct improved their score (starting from 6–11.5 and reaching final scores 10–17.5) while 25% remained at the same level (score 8–7). In the saline and LHM group no improvement was detected (score between 9–11 and 7–9 respectively). In the plantar test, a non-significant decrease in latency to thermal nociceptive stimulus was observed during the study, however, this was not considered to be causing additional hyperalgesia (Fig. 8B).

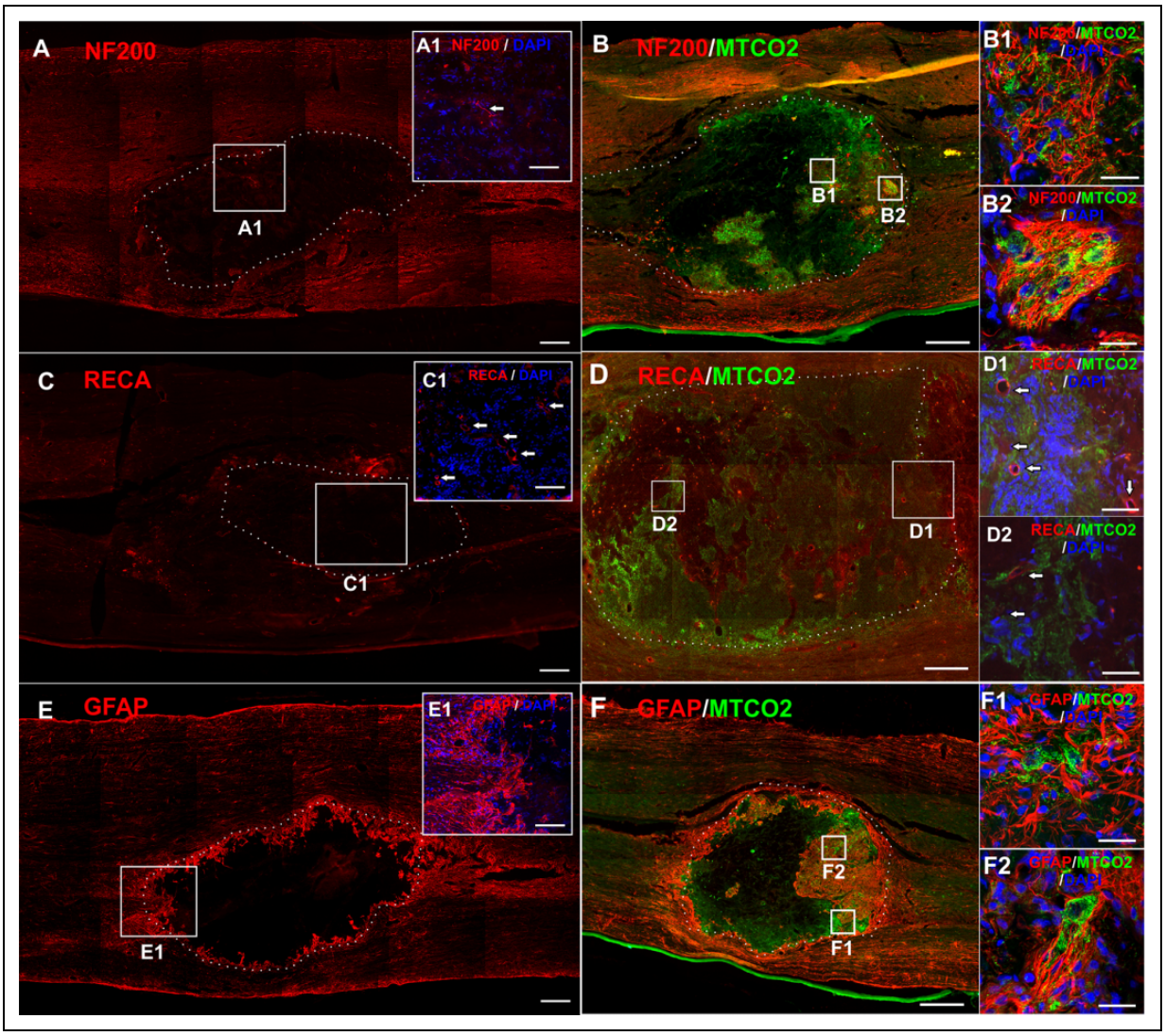

Fig. 5. Immunohistochemistry showing the tissue element incorporation into an implanted LHM hydrogel without (A, C, E) or with iPSC-NPs (B, D, F), 28 weeks after SCI. Almost no ingrowth of axons (NF200, red, A, detail A1) was observed into the implanted LHM gel without cells. On the contrary, an implanted cell-polymer construct was infiltrated with cells that survived and endogenous axons (NF200, red B, detail B1, 2). Blood vessels infiltrated gels with or without cells (RECA, red, C, D, detail C1, D1, D2). The implanted hydrogel was always surrounded with a GFAP-positive glial scar (GFAP, red, E, F). GFAP-positive cells were found within the hydrogel in close vicinity with implanted stem cells (detail F1, 2). Human iPSC-NPs were stained with MTC02 (green). Nuclei were stained with DAPI (blue). Scale bars are 500 μm (A, B, E, F), 400 μm (C, D), 40 μm (C1, D1, 2) and 20 μm (A1, B1, 2, E1, F1, 2).
DAPI: 4', 6-2, dihydrochloride; GFAP: glial fibrillary acidic protein; iPSC-NP: induced pluripotent stem cell-derived neural progenitor; LHM: laminin-coated pHEMA-MOETACl; SCI: spinal cord injury.

Discussion

In our study, the combined therapy using LHM hydrogel seeded with iPSC-NPs showed the ability of the cell-polymer construct to bridge the lesion, integrate into the host tissue, and support implant vascularization and ingrowth of axons and GFAP-positive astrocytes, from the injured spinal cord into the implant. Scaffold seeded with iPSC-NPs, affected the number of endogenous TH^+ neurons and closely communicated with endogenous axons and astrocytes. However, these changes did not lead to behavioral recovery of chronic SCI.

Combined therapies using stem cells and/or biomaterials are often used in the treatment of acute SCI with a positive outcome[31,32].

In the current study, immunohistochemical analysis, as well as diffusion measurements in vitro were performed prior to in vivo transplantation to assess the biocompatibility and suitable physical properties of the chosen hydrogel. Immunohistological evaluation showed that LHM hydrogel is a very feasible material supporting the growth and proliferation of seeded iPSC-NPs, and confirmed that the cells adhere and spread over the biomaterial. The diffusion

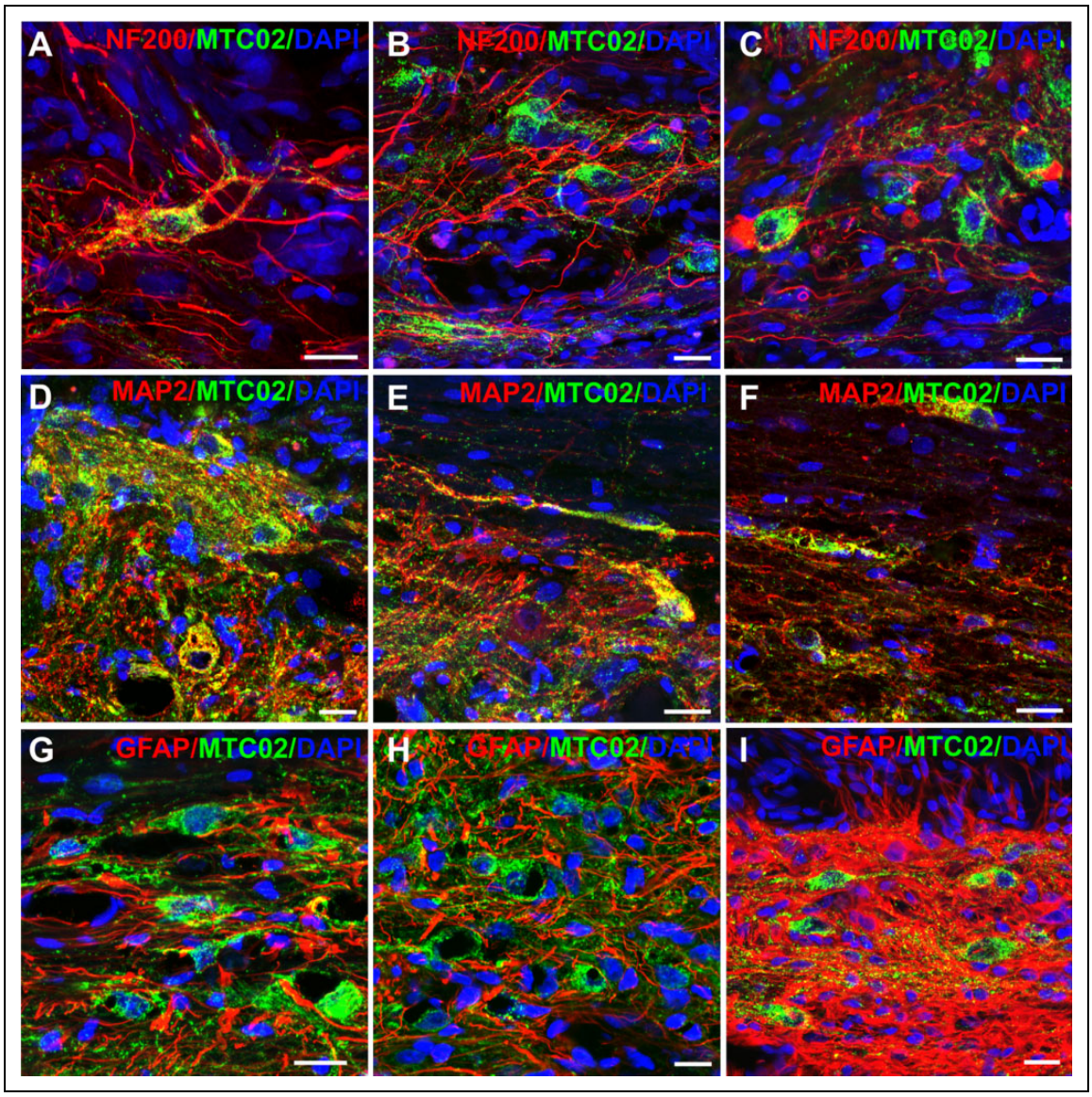

Fig. 6. Survival and differentiation of iPSC-NPs outside the hydrogel 28 weeks after SCI. iPSC-NPs that migrated out of the LHM hydrogel, differentiated into NF200 (A–C) and MAP2 (D–F) positive cells. Most of the cells with neuron-like morphology were not positive for GFAP (G–I). Images were taken from three different animals. All the scale bars are 20 μm.
GFAP: glial fibrillary acidic protein; iPSC-NP: induced pluripotent stem cell-derived neural progenitor; LHM: laminin-coated pHEMA-MOETACl; MAP2: microtubule-associated protein 2; SCI: spinal cord injury.

measurements detected small changes in the diffusion properties associated with cell seeding but even 3 weeks after cell seeding, volume fraction remained more than twice as high as in the immature tissue[33,34], leaving enough space in the hydrogel pores to support the ingrowth of spinal cord tissue elements, and the diffusion of nutrition and growth factors.

At 3 weeks after seeding, the cells showed a rather immature but typical neural progenitor phenotype. The laminin coating supported the attachment and growth of cells in the hydrogel but did not facilitate their differentiation. The cells remained immature, mostly positive for nestin and olig2 with only a minority being MAP2 or GFAP positive. On the other hand, the cells did not show a stress related phenotype, and populated the whole area of the hydrogel. The HEMA-MOETACl hydrogel with a surface modified with serotonin molecules (HEMA-5HT) was used in combination with a fetal spinal progenitor cell line (SPC-01) in our previous study[35]. In in vitro experiments, after 3 weeks growing in hydrogel, SPC-01, the cells were positive for synaptophysin and β-III tubulin, forming neuronal nets within the scaffold. Growth in vitro unfortunately, does not reflect the situation in vivo. The environment of chronically injured nervous tissue is a great challenge for neural progenitor survival, growth and differentiation. Scaffolds that are robustly

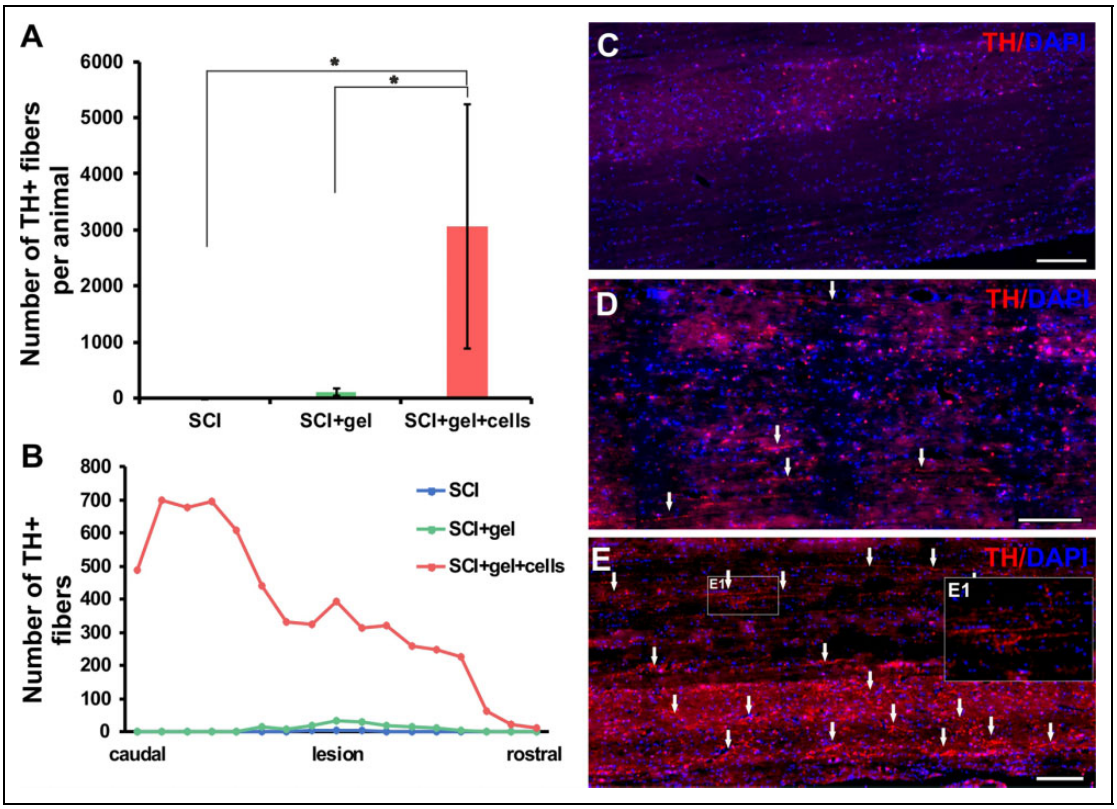

Fig. 7. Density and distribution of TH-positive fibers in the injured spinal cords of control rats (n=4), and rats transplanted with gel (n=3) and gel seeded with iPSC-NPs (n=4). From each animal at least 8–10 slides were analyzed. (A) Quantitative analysis of the number of TH-positive fibers in the spinal cord tissue of control and transplanted animals. (B) Distribution of TH-positive fibers in the spinal cord tissue of control and transplanted animals. (C) Histochemical staining demonstrates the different density of TH-positive fibers in the injured spinal cord. (D) Injured spinal cord transplanted with gel only and (E) transplanted with iPSC-NP-seeded gel (detail of TH^+fiberE1). All the scale bars are 200 μm.
iPSC-NP: induced pluripotent stem cell-derived neural progenitor; TH: tyrosine hydroxylase.

populated with cells in vitro, do not necessarily serve as an ideal cell carrier for an in vivo hostile environment. LHM hydrogels supported the adhesion and growth of cells in the material for the whole period of study (28 weeks), however the cells remained in a rather immature stage and exerted their influence on tissue regeneration mainly via the paracrine effect. The same cells, when grafted into SCI in its acute phase, survived over four months and differentiated and matured into dopaminergic, serotonergic, GABAergic and motor neurons[19]. In this study, the cells that were in contact with host neural tissue displayed a neuronal phenotype, although they did not mature into tissue-specific neurons. The modified environment in the chronic phase of the injury seems to negatively influence their maturation and differentiation. No functional improvement was described after the grafting of caudalized human iPSC-NPs into cervical chronic SCI, even though the cells were able to produce neurons and glia[15]. However, the cell-polymer construct has strongly affected the lateral sprouting of TH^+ axons within the injured region, as well as alongside them, when compared with the application of both LHM hydrogel and saline-treated animals. The amount of TH^+ axons did not correlate with a decreased latency to nociceptive thermal stimulus in individual animals, and on the contrary, animals with a high number of TH^+ axons showed the opposite trend. More importantly, it has been described that an increased input of TH^+ axons could lead to improved urinary bladder function after SCI[36,37]. We did not observe any tumor formation or hyperproliferation in any of our studies, in which we used these iPSC-NPs. We did not count $Ki67^+$ cells in these settings, however, in acute SCI and in the rat stroke model we detected less than 3% of Ki67 positive cells in the grafts[19,27].

Different stem cells, in combination with biomaterial, growth factors or chondroitinase, were tested in chronic models of SCI[29,38–41]. In some studies, good cell survival, differentiation, production of growth factors and cytokines, but only modest or no functional improvement was observed in chronic settings[41–43]. A successful combined therapy used directly reprogrammed human NPs, biased toward an oligodendrogenic fate (oNPs), in combination with the sustained delivery of enzyme chondroitinase ABC released in the crosslinked methylcellulose biomaterial in a rat

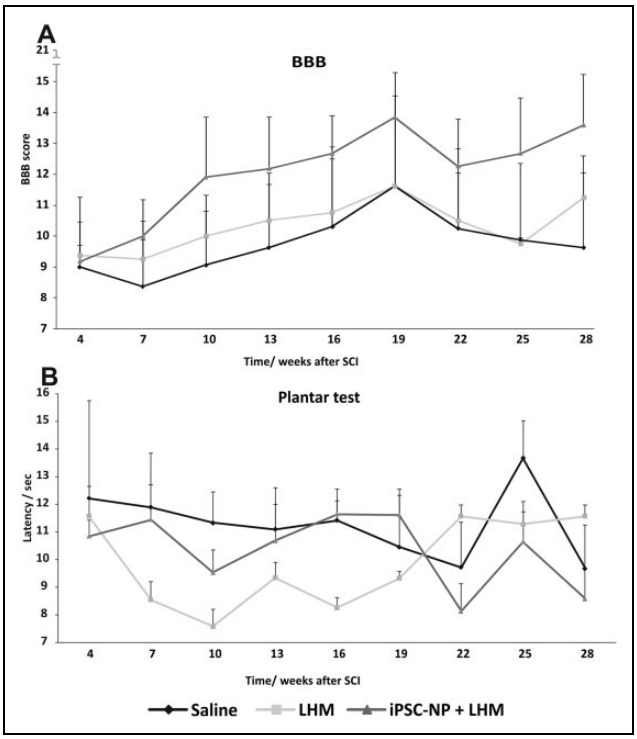

Fig. 8. Functional recovery after LHM + iPSC-NP combined treatment of chronic SCI. No significant differences were found between all tested groups, neither in motoric recovery (BBB test, A), nor in thermal nociceptive stimulus (plantar test, B).
BBB: Basso, Beattie, and Bresnahan; iPSC-NP: induced pluripotent stem cell-derived neural progenitor; LHM: laminin-coated pHEMA-MOETACl; SCI: spinal cord injury.

immunodeficient model. This combinatorial therapy increased the long-term survival of oNPs around the lesion epicenter, facilitated greater oligodendrocyte differentiation, remyelination of the spared axons by engrafted oNPs and enhanced synaptic connectivity with anterior horn cells and neurobehavioral recovery[44]. Locomotor improvement has also been described in studies, utilizing collagen scaffold (NeuroRegen) seeded with MSCs in rats and dogs[45]. Improved cortical motor- and somatosensory-evoked potentials were observed in rats[46]. Due to the high variability in the scores 5 weeks after injury (implantation time), we cannot draw any conclusions about the functional outcome. We observed a trend in improvement in 75% of animals up to 19 weeks after SCI, however, after this time point, a stagnation or even a slight decline was observed. This might be prevented by physical exercise during the experiment, such as treadmill sessions. The muscle atrophy and weight gain could have negatively affected the overall functional outcome.

It is clear that although the integration of the scaffold and neural differentiation of grafted cells did not result in functional recovery, it could modify the chronic environment and potentially lead to important physiological function restoration. Therapies using modified stem cells or combined therapies of stem cells, peripheral grafts or chondroitinase and growth factors, suggest that there is still remaining plasticity which can be enhanced to support some regeneration and/or behavioral recovery after chronic SCI.

Conclusion

The implantation of the iPSC-NP-LHM cell-polymer construct into the chronic SCI led to the integration of material into the injured spinal cord, and reduced cavitation with no negative impact on the treated animals. The iPSC-NPs survived in the scaffold throughout the whole study, and positively influenced the number of endogenous TH^+ neurons. Contrary to excellent in vitro properties, the iPSC-NP-LHM construct showed only partial effectivity in the severe chronic SCI, and further co-therapies that will augment the efficacy of neural cell transplant and restore function in chronic SCI, have to be identified.

Acknowledgements

MRI scans of spinal cord prior the implantation of LHM hydrogel were prepared in collaboration with Martin Burian from the Radiology Department of the Institute for Clinical and Experimental Medicine (IKEM). Research data for TH analysis were collected in cooperation with Ivan Kanchev, DVM of the Czech Centre for Phenogenomics, supported by the Academy of Sciences of the Czech Republic RVO 68378050 under the project of the support program for large infrastructures for research, experimental development and innovation LM2015040; Czech Centre for Phenogenomics, and by the project of the National Program of Sustainability II LQ1604, both provided by the Ministry of Education, Youth and Sports of the Czech Republic.

Author Contribution

Pavla Jendelova designed the study and wrote the manuscript. Jiri Ruzicka performed the injury model, behavioral tests and wrote the manuscript. Ales Hejcl and Lucia Urdzikova implanted the material and stem cells. Klara Jirakova cultivated and seeded the iPSC-NP and evaluated the in vitro part of the study. Nataliya Romanyuk analyzed in vivo fate of implanted iPSC-NP. Martin Pradny and Olga Janouskova prepared the LHM hydrogel. Marcel Bochin performed the ECS and tortuosity measurements. Lydia Vargova interpreted and analyzed the diffusion measurements data.

Ethical Approval

This study was approved by the Ethics Committee of the Institute of Experimental Medicine, Academy of Sciences of the Czech Republic.

Statement of Human and Animal Rights

All experiments were performed in accordance with the European Communities Council Directive of 22 September 2010 (2010/63/EU) regarding the use of animals in research.

Statement of Informed Consent

There are no human subjects in this article and informed consent is not applicable.

Declaration of Conflicting Interests

The author(s) declared no potential conflicts of interest with respect to the research, authorship, and/or publication of this article.

Funding

The author(s) disclosed receipt of the following financial support for the research, authorship, and/or publication of this article: This work was supported by grant Czech National Foundation 17-11140S, by the European Union, the Operational Programme of Research, Development and Education under the framework of the project "Centre of Reconstructive Neuroscience", registration number CZ.02.1.01/0.0./0.0/15_003/0000419.

References

1. Sekhon LH, Fehlings MG. Epidemiology, demographics, and pathophysiology of acute spinal cord injury. Spine (Phila Pa 1976). 2001;26(24 Suppl):S2–S12.
2. Fawcett JW. The glial response to injury and its role in the inhibition of CNS repair. Adv Exp Med Biol. 2006;557:11–24.
3. Schwab ME. Increasing plasticity and functional recovery of the lesioned spinal cord. Prog Brain Res. 2002;137:351–359.
4. Amemori T, Jendelová P, Ruzickova K, Arboleda D, Syková E. Co-transplantation of olfactory ensheathing glia and mesenchymal stromal cells does not have synergistic effects after spinal cord injury in the rat. Cytotherapy. 2010;12(2): 212–225.
5. Arboleda D, Forostyak S, Jendelová P, Marekova D, Amemori T, Pivonkova H, Masinova K, Syková E. Transplantation of predifferentiated adipose-derived stromal cells for the treatment of spinal cord injury. Cell Mol Neurobiol. 2011;31(7): 1113–1122.
6. Coutts M, Keirstead HS. Stem cells for the treatment of spinal cord injury. Exp Neurol. 2008;209(2):368–377.
7. Urdzikova L, Jendelová P, Glogarova K, Burian M, Hájek M, Syková E. Transplantation of bone marrow stem cells as well as mobilization by granulocyte-colony stimulating factor promotes recovery after spinal cord injury in rats. J Neurotrauma. 2006;23(9):1379–1391.
8. Urdzikova L, Likavcanová-mašínová K, Vanecek V, Ruzicka J, Sedý J, Syková E, Jendelová P. Flt3 ligand synergizes with granulocyte-colony-stimulating factor in bone marrow mobilization to improve functional outcome after spinal cord injury in the rat. Cytotherapy. 2011;13(9):1090–1104.
9. Ruff CA, Wilcox JT, Fehlings MG. Cell-based transplantation strategies to promote plasticity following spinal cord injury. Exp Neurol. 2012;235(1):78–90.
10. Wilcox JT, Satkunendrarajah K, Zuccato JA, Nassiri F, Fehlings MG. Neural precursor cell transplantation enhances functional recovery and reduces astrogliosis in bilateral compressive/contusive cervical spinal cord injury. Stem Cells Transl Med. 2014;3(10):1148–1159.
11. Urdzikova LM, Ruzicka J, LaBagnara M, Karova K, Kubinova S, Jirakova K, Murali R, Syková E, Jhanwar-Uniyal M, Jendelová P. Human mesenchymal stem cells modulate inflammatory cytokines after spinal cord injury in rat. Int J Mol Sci. 2014;15(7):11275–11293.
12. Kawabata S, Takano M, Numasawa-Kuroiwa Y, Itakura G, Kobayashi Y, Nishiyama Y, Sugai K, Nishimura S, Iwai H, Isoda M, Shibata S, Kohyama J, Iwanami A, Toyama Y, Matsumoto M, Nakamura M, Okano H. Grafted human iPS cell-derived oligodendrocyte precursor cells contribute to robust remyelination of demyelinated axons after spinal cord injury. Stem Cell Reports. 2016;6(1):1–8.
13. Takahashi K, Yamanaka S. Induction of pluripotent stem cells from mouse embryonic and adult fibroblast cultures by defined factors. Cell. 2006;126(4):663–676.
14. Kobayashi Y, Okada Y, Itakura G, Iwai H, Nishimura S, Yasuda A, Nori S, Hikishima K, Konomi T, Fujiyoshi K, Tsuji O, Toyama Y, Yamanaka S, Nakamura M, Okano H. Pre-evaluated safe human iPSC-derived neural stem cells promote functional recovery after spinal cord injury in common marmoset without tumorigenicity. PLoS One. 2012;7(12):e52787.
15. Nutt SE, Chang EA, Suhr ST, Schlosser LO, Mondello SE, Moritz CT, Cibelli JB, Horner PJ. Caudalized human iPSC-derived neural progenitor cells produce neurons and glia but fail to restore function in an early chronic spinal cord injury model. Exp Neurol. 2013;248:491–503.
16. Sareen D, Gowing G, Sahabian A, Staggenborg K, Paradis R, Avalos P, Latter J, Ornelas L, Garcia L, Svendsen CN. Human induced pluripotent stem cells are a novel source of neural progenitor cells (iNPCs) that migrate and integrate in the rodent spinal cord. J Comp Neurol. 2014;522(12):2707–2728.
17. Tsuji O, Miura K, Fujiyoshi K, Momoshima S, Nakamura M, Okano H. Cell therapy for spinal cord injury by neural stem/progenitor cells derived from iPS/ES cells. Neurotherapeutics. 2011;8(4):668–676.
18. Prádný M, Duskova-Smrckova M, Dusek K, Janouskova O, Sadakbayeva Z, Slouf M, Michálek J. Macroporous 2-hydroxyethyl methacrylate hydrogels of dual porosity for cell cultivation: morphology, swelling, permeability, and mechanical behavior. J Polym Res. 2014;21(11):579.
19. Romanyuk N, Amemori T, Turnovcova K, Prochazka P, Onteniente B, Syková E, Jendelová P. Beneficial effect of human induced pluripotent stem cell-derived neural precursors in spinal cord injury repair. Cell Transplant. 2015;24(9): 1781–1797.
20. Ruzicka J, Machova-Urdzikova L, Gillick J, Amemori T, Romanyuk N, Karova K, Zaviskova K, Dubisova J, Kubinova S, Murali R, Syková E, Jhanwar-Uniyal M, Jendelová P. A comparative study of three different types of stem cells for treatment of rat spinal cord injury. Cell Transplant. 2017;26(4):585–603.
21. Hejcl A, Ruzicka J, Kapcalová M, Turnovcova K, Krumbholcová E, Prádný M, Michálek J, Cihlar J, Jendelová P, Syková E. Adjusting the chemical and physical properties of hydrogels leads to improved stem cell survival and tissue ingrowth in spinal cord injury reconstruction: a comparative study of four methacrylate hydrogels. Stem Cells Dev. 2013;22(20):2794–2805.
22. Prádný M, Lesný P, Smetana K Jr, Vacik J, Slouf M, Michálek J, Syková E. Macroporous hydrogels based on 2-hydroxyethyl methacrylate. Part II. Copolymers with positive and negative charges, polyelectrolyte complexes. J Mater Sci Mater Med. 2005;16(8):767–773.

23. Nicholson C, Phillips JM. Ion diffusion modified by tortuosity and volume fraction in the extracellular microenvironment of the rat cerebellum. J Physiol. 1981;321:225–257.
24. Syková E.Ionic and Volume Changes in the Microenvironment of Nerve and Receptor Cells. New York (NY): Springer-Verlag; 1992. p. 1–167.
25. Syková E, Nicholson C. Diffusion in brain extracellular space. Physiol Rev. 2008;88(4):1277–1340.
26. Yu J, Vodyanik MA, Smuga-Otto K, Antosiewicz-Bourget J, Frane JL, Tian S, Nie J, Jonsdottir GA, Ruotti V, Stewart R, Slukvin II, Thomson JA. Induced pluripotent stem cell lines derived from human somatic cells. Science. 2007;318(5858): 1917–1920.
27. Polentes J, Jendelová P, Cailleret M, Braun H, Romanyuk N, Tropel P, Brenot M, Itier V, Seminatore C, Baldauf K, Turnovcova K, Jirak D, Teletin M, Côme J, Tournois J, Reymann K, Syková E, Viville S, Onteniente B. Human induced pluripotent stem cells improve stroke outcome and reduce secondary degeneration in the recipient brain. Cell Transplant. 2012; 21(12):2587–2602.
28. Vanicky I, Urdzikova L, Saganova K, Cizkova D, Galik J. A simple and reproducible model of spinal cord injury induced by epidural balloon inflation in the rat. J Neurotrauma. 2001; 18(12):1399–1407.
29. Hejcl A, Sedý J, Kapcalová M, Toro DA, Amemori T, Lesný P, Likavcanová-Mašínová K, Krumbholcová E, Pradny M, Michálek J, Burian M, Hájek M, Jendelová P, Syková E. HPMA-RGD hydrogels seeded with mesenchymal stem cells improve functional outcome in chronic spinal cord injury. Stem Cells Dev. 2010;19(10):1535–1546.
30. Basso DM, Beattie MS, Bresnahan JC. A sensitive and reliable locomotor rating scale for open field testing in rats. J Neurotrauma. 1995;12(1):1–21.
31. Fan C, Li X, Zhao Y, Xiao Z, Xue W, Sun J, Zhuang Y, Chen Y, Dai J. Cetuximab and Taxol co-modified collagen scaffolds show combination effects for the repair of acute spinal cord injury. Biomater Sci. 2018;6(7):1723–1734.
32. Zweckberger K, Liu Y, Wang J, Forgione N, Fehlings MG. Synergetic use of neural precursor cells and self-assembling peptides in experimental cervical spinal cord injury. J Vis Exp. 2015;(96):e52105.
33. Lehmenkuhler A, Syková E, Svoboda J, Zilles K, Nicholson C. Extracellular space parameters in the rat neocortex and subcortical white matter during postnatal development determined by diffusion analysis. Neuroscience. 1993; 55(2):339–351.
34. Vorisek I, Syková E. Evolution of anisotropic diffusion in the developing rat corpus callosum. J Neurophysiol. 1997;78(2): 912–919.
35. Ruzicka J, Romanyuk N, Hejcl A, Vetrik M, Hruby M, Cocks G, Cihlar J, Prádný M, Price J, Syková E, Jendelová P. Treating spinal cord injury in rats with a combination of human fetal neural stem cells and hydrogels modified with serotonin. Acta Neurobiol Exp (Wars). 2013;73(1): 102–115.
36. Lee YS, Lin CY, Jiang HH, Depaul M, Lin VW, Silver J. Nerve regeneration restores supraspinal control of bladder function after complete spinal cord injury. J Neurosci. 2013;33(26): 10591–10606.
37. Ryu JC, Tooke K, Malley SE, Soulas A, Weiss T, Ganesh N, Saidi N, Daugherty S, Saragovi U, Ikeda Y, Zabbarova I, Kanai AJ, Yoshiyama M, Farhadi HF, de Groat WC, Vizzard MA, Yoon SO. Role of proNGF/p75 signaling in bladder dysfunction after spinal cord injury. J Clin Invest. 2018;128(5): 1772–1786.
38. Amr SM, Gouda A, Koptan WT, Galal AA, Abdel-Fattah DS, Rashed LA, Atta HM, Abdel-Aziz MT. Bridging defects in chronic spinal cord injury using peripheral nerve grafts combined with a chitosan-laminin scaffold and enhancing regeneration through them by co-transplantation with bone-marrow-derived mesenchymal stem cells: case series of 14 patients. J Spinal Cord Med. 2014;37(1):54–71.
39. Barakat DJ, Gaglani SM, Neravetla SR, Sanchez AR, Andrade CM, Pressman Y, Puzis R, Garg MS, Bunge MB, Pearse DD. Survival, integration, and axon growth support of glia transplanted into the chronically contused spinal cord. Cell Transplant. 2005;14(4):225–240.
40. Tom VJ, Sandrow-Feinberg HR, Miller K, Santi L, Connors T, Lemay MA, Houle JD. Combining peripheral nerve grafts and chondroitinase promotes functional axonal regeneration in the chronically injured spinal cord. J Neurosci. 2009;29(47): 14881–14890.
41. Nomura H, Baladie B, Katayama Y, Morshead CM, Shoichet MS, Tator CH. Delayed implantation of intramedullary chitosan channels containing nerve grafts promotes extensive axonal regeneration after spinal cord injury. Neurosurgery. 2008; 63(1):127–141; discussion 141–143.
42. Jin Y, Bouyer J, Shumsky JS, Haas C, Fischer I. Transplantation of neural progenitor cells in chronic spinal cord injury. Neuroscience. 2016;320:69–82.
43. Kumamaru H, Saiwai H, Kubota K, Kobayakawa K, Yokota K, Ohkawa Y, Shiba K, Iwamoto Y, Okada S. Therapeutic activities of engrafted neural stem/precursor cells are not dormant in the chronically injured spinal cord. Stem Cells. 2013;31(8): 1535–1547.
44. Nori S, Khazaei M, Ahuja CS, Yokota K, Ahlfors JE, Liu Y, Wang J, Shibata S, Chio J, Hettiaratchi MH, Führmann T, Shoichet MS, Fehlings MG. Human oligodendrogenic neural progenitor cells delivered with chondroitinase ABC facilitate functional repair of chronic spinal cord injury. Stem Cell Reports. 2018;11(6):1433–1448.
45. Wang N, Xiao Z, Zhao Y, Wang B, Li X, Li J, Dai J. Collagen scaffold combined with human umbilical cord-derived mesenchymal stem cells promote functional recovery after scar resection in rats with chronic spinal cord injury. J Tissue Eng Regen Med. 2018;12(2):e1154–e1163.
46. Li X, Tan J, Xiao Z, Zhao Y, Han S, Liu D, Yin W, Li J, Li J, Wanggou S, Chen B, Ren C, Jiang X, Dai J. Transplantation of hUC-MSCs seeded collagen scaffolds reduces scar formation and promotes functional recovery in canines with chronic spinal cord injury. Sci Rep. 2017;7:43559.